Superelastic shape memory alloy cables: Part II – Subcomponent isothermal responses

Benjamin Reedlunn [a,*], Samantha Daly [b,c], John Shaw [d]

[a] Sandia National Laboratories, P.O. Box 5800, Albuquerque, NM 87185, USA
[b] University of Michigan, Dept. of Mechanical Engineering, 2350 Hayward St., Ann Arbor, MI 48109, USA
[c] University of Michigan, Dept. of Materials Science and Engineering, 2300 Hayward St., Ann Arbor, MI 48109, USA
[d] University of Michigan, Dept. of Aerospace Engineering, 1320 Beal Ave., Ann Arbor, MI 48109, USA

ABSTRACT

This paper constitutes the second part of our experimental study of the thermo-mechanical behavior of superelastic NiTi shape memory alloy cables. Part I introduced the fundamental, room temperature, tensile responses of two cable designs (7×7 right regular lay, and 1×27 alternating lay). In Part II, each cable behavior is studied further by breaking down the response into the contributions of its hierarchical subcomponents. Selected wire strands were extracted from the two cable constructions, and their quasi-static tension responses were measured using the same experimental setup of Part I. Consistent with the shallow wire helix angles in the 7×7 construction, the force–elongation responses of the core wire, 1×7 core strand and full 7×7 cable were similar on a normalized basis, with only a slight decrease in transformation force plateaus and slight increase in plateau strains in this specimen sequence. By contrast, each successive 1×27 component (1×6 core strand, 1×15 strand, and full cable) included an additional outer layer of wires with a larger number of wires, greater helix radius, and deeper helix angle, so the normalized axial load responses became significantly more compliant. Each specimen in the sequence also exhibited progressively larger strains at failure, reaching 40% strain in the full 1×27 cable.

Stress-induced phase transformations involved localized strain/temperature and front propagation in all of the tested 7×7 components but none of the 1×27 components aside from the 1×27 core wire. Stereo digital image correlation measurements revealed finer features within a global transformation front of the 1×7 core strand than the 7×7 cable, consisting of an staggered pattern of individual wire fronts that moved in lock-step during elongation. Although the 1×27 multi-layer strands exhibited temperature/strain localizations in a distributed pattern during transformations, the localizations did not propagate and their cause was traced back to contact indentations (stress concentrations) arising from the cable's fabrication. The normalized axial torque responses of the multi-layer 1×27 components during transformation were distinctly non-monotonic and complex, due to the alternating handedness of the layers. Force and torque contributions of individual wire layers were deduced by subtracting 1×27 component responses, which helped to clarify the transformation kinetics within each layer and explain the unusual force and torque undulations seen in the 1×27 cable response of Part I.

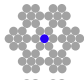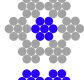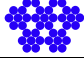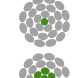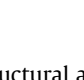© 2013 Elsevier Ltd. All rights reserved.

1. Introduction

This is the second article of our two-part series exploring the tensile response of superelastic shape memory alloy (SMA) cables. Part I (Reedlunn et al., 2013) reviewed the construction of typical structural cables (wire ropes) and described how SMA wire in cable form combines the attractive properties of structural cables (redundant load carrying and spooling for compact packing) with the adaptive characteristics of SMAs (shape memory and super-

elasticity). Besides these independent features, the combination has additional synergetic advantages (tailorable structural performance, reduced thermal lag, and ease of manufacture for large force applications) that make a characterization study of SMA cables of both scientific and engineering interest. Two SMA cable designs, a 7×7 right regular lay and a 1×27 alternating lay, constructed of superelastic NiTi wires (as received from Ft. Wayne Metals Research) were described and characterized. A custom experimental setup, involving infrared (IR) thermography and stereo digital image correlation (DIC), examined the isothermal, superelastic responses of the two designs. The two cable designs exhibited quite different thermomechanical responses, spanning a range of superelastic behaviors, each of which might be advanta-

Table 1
Specimen components from two cable designs and experimental and geometric parameters

Cable	Specimen	Icon	A_0 (mm^2)	J_0/R (mm^3)	Exp ID	L (mm)	L_e (mm)	$\dot{\delta}/L$ (s^{-1})
	Core wire		0.059	4.083×10^{-3}	W1b	76.04	49.55	$\pm 1 \times 10^{-5}$
7×7	1×7 Core strand		0.416	7.486×10^{-2}	S1a	75.93	50.17	$\pm 1 \times 10^{-5}$
	7×7 Cable		2.910	1.547×10^{0}	C1c	74.85	49.92	$\pm 1 \times 10^{-5}$
	Core wire		0.040	2.266×10^{-3}	W2b	74.67	49.05	$\pm 1 \times 10^{-4}$
	1×6 Core strand		0.241	3.475×10^{-2}	S2a	75.05	49.70	$\pm 1 \times 10^{-4}$
1×27	1×15 multi-layer		0.602	1.555×10^{-1}	M2a	75.09	49.88	$\pm 1 \times 10^{-4}$
	1×27 Cable		1.083	3.947×10^{-1}	C2d	75.21	49.21	$\pm 1 \times 10^{-4}$

geous depending on the intended structural application. The 7×7 cable performed similar to forty-nine NiTi wires pulled in parallel, and stress-induced transformations (both $A \to M^+$ during loading and $M^+ \to A$ during unloading) involved propagating transformation fronts as typically seen in straight NiTi wires. On the other hand, the 1×27 cable exhibited a significantly more compliant response, no propagating transformation fronts, and an intriguing axial torque response. In addition, the cyclic responses of the two designs were quite different, with less severe shakedown generally occurring in the 1×27 cable.

While Part I introduced the two designs by comparing their baseline performance, it raised a number of questions, especially for the 1×27 design. Here in Part II, we focus again on the same two cable designs and explore the isothermal response of selected subcomponents excised from each cable construction in an effort to explain the observed behavior of the full cables. It is also worthwhile to characterize the underlying components as a matter of scientific curiosity, and for the simple reason that certain applications may utilize the individual cable components as structural elements in their own right. The intended scope of this article is largely experimental and descriptive. For now, we leave the interesting topic of detailed structural modeling for future work and confine ourselves to simple analyses as needed to explain observed phenomena.

This article is organized as follows. Section 2 provides a summary of the experimental scope, focusing on the room temperature superelastic behavior of individual components at nearly isothermal elongation rates. Section 2 also provides further details on the geometry of the helical wires used in the cable designs. Section 3 provides a comparison of responses of three selected components in the 7×7 design, and provides experimental results showing further detail and new features of propagating transformation fronts in the straight core wire and the 1×7 core strand. Section 4 provides experimental responses of four selected components of the 1×27 construction, which help to explain the overall enhanced compliance of the full cable, the lack of localized self heating/cooling, the multi-knee force response, and the interesting "stair-step" torque response. Section 4 also provides a breakdown of the individual layer-by-layer responses, deduced by subtracting the components' measured force and torque responses from one another.

2. Experimental scope & specimen details

The $7 \times 7 \times 0.275$ mm and $1 \times 27 \times 0.226$ mm cable designs, and their selected components used in this experimental study, are shown in Table 1. All specimens came from the same two cable lots utilized in Part I, and when necessary, the cables were disassembled to extract individual components for testing. The components shown in Table 1 are the set of nominally straight specimens that could be excised from the full cables: three for the 7×7 cable and four for the 1×27 cable. (All other possible components involved helical elements that would be much more challenging to test experimentally.) The experiments on the straight core wires and the full cables were presented in Part I; here we have added the intermediate components to study the complete hierarchy in the respective cable constructions. As before, specimens were lightly painted with a specular pattern to allow DIC measurements and to increase the emissivity of the surface for IR imaging, and reflective tags were attached to allow laser extensometry.

The same experimental setup as in Part I was utilized for the experiments presented in this paper. All experiments were performed on new, dry specimens in room temperature air. The lower grip was held fixed and the upper grip was displaced upward by a mechanical testing machine to stretch the specimen under elongation control at constant, slow ramp rates ($\dot{\delta}/L$) while monitoring the axial load. The grips rigidly clamped the specimen at its ends to enforce zero-rotation boundary conditions, and the resultant axial reaction torque was measured using a torque cell. In certain cases, stereo DIC was performed to measure the strain field evolution (in a restricted field of view) and infrared (IR) imaging was performed to measure the temperature field transients. Mechanical responses are presented in terms of the normalized axial load (P/A_0, axial force per reference area) and normalized axial torque ($M_z R/J_0$, axial moment times outer radius per reference torsion constant). The chosen reference area (A_0) and reference torsion constant (J_0/R) were defined in Section 5 of Part I, and values are provided for each component being examined in Table 1. Sections 3 and 4 will present the respective experimental results and analyses of the component responses for the two cable types, 7×7 and 1×27. Responses are generally plotted either against the laser extensometer (LE) gage strain (δ_e/L_e) or time (t).